

Island Shape Selection in Pt(111) Submonolayer Homoepitaxy with or without CO as an Adsorbate

Jing Wu,¹ E. G. Wang,^{1,2} K. Varga,³ B. G. Liu,¹ S. T. Pantelides,^{3,4} and Zhenyu Zhang^{3,2}

¹*Institute of Physics, Chinese Academy of Sciences, Beijing 100080, People's Republic of China*

²*International Center for Quantum Structures, Chinese Academy of Sciences, Beijing 100080, People's Republic of China*

³*Solid State Division, Oak Ridge National Laboratory, Oak Ridge, Tennessee 37831-6032*

⁴*Department of Physics, Vanderbilt University, Nashville, Tennessee 37235*

(Received 21 April 2000; revised manuscript received 9 August 2001; published 16 September 2002)

The microscopic selection mechanisms of single-layer island shapes in Pt(111) homoepitaxy with or without minute amounts of CO adsorbate have been investigated theoretically. For clean growth, only triangular islands of a fixed orientation are obtained within a wide range of growth temperatures, with the orientation uniquely determined by a disparity in the rates of atom supply to an island corner site from the two island edges defining the corner. This novel picture is further corroborated by growth predictions in the presence of CO, whose preferential decoration of one type of the island edges reverses the intrinsic rate disparity for atom supply, thereby inverting the island orientation.

DOI: 10.1103/PhysRevLett.89.146103

PACS numbers: 68.35.Bs, 68.35.Fx, 68.55.Ln

Understanding the microscopic mechanisms involved in thin-film growth has been an active area of research over the years. In these studies, Pt(111) homoepitaxy as a model system has received particular attention [1–4]. In the earliest stages of Pt(111) homoepitaxy where only single-layer islands are formed, Michely *et al.* found that the islands develop fractal or dendritic shapes at low growth temperatures but are compact at higher temperatures [2]. Most intriguingly, the compact islands can select triangular, hexagonal, inverted triangular, and re-entrant hexagonal shapes as the growth temperature is increased. This set of observations has defied a consensus explanation for years [2,5–8]. The chance of eventual identification of the missing microscopic mechanisms was greatly enhanced by the unexpected new finding of a new experiment [3], in which the same group traced the origin of the shape evolution to the effects of low concentrations of adsorbed CO in the growth system. Despite this new finding, the precise atomistic mechanisms for the selection of a particular island shape and orientation in Pt(111) homoepitaxy remain to be explored. Earlier theoretical studies had been restricted primarily to the case of clean Pt(111) homoepitaxy, and various schemes had been proposed to explain the intriguing observations of the island shape transitions [2,5–8]. Nevertheless, in every earlier attempt, central conclusions had been drawn with the use of key simulation parameters that were either from empirical interatomic potentials, or simply freely adjustable, making it difficult to assess the validity of each picture, let alone to differentiate between them.

In this Letter, we provide a coherent and unified picture for the selection of two-dimensional island shapes in Pt(111) homoepitaxy without or with the presence of minute amounts of CO adsorbates, as obtained by kinetic Monte Carlo (KMC) simulations. For clean growth, we rigorously adopt the energy barriers from Feibelman's

first-principles calculations for Pt/Pt(111) [9] and show that only triangular islands with a fixed orientation are obtained within a wide range of growth temperatures. The orientation of the triangular islands is uniquely determined by a disparity in the rates of atom supply to an island corner site from the two island edges defining the island corner. This picture is further corroborated by predictions of island shape evolution in the presence of CO, whose preferential decoration of one type of the island edges reverses the intrinsic rate disparity for atom supply, thereby inverting the island orientation.

There are two types of close-packed steps on the (111) surface of fcc metals such as Pt: the (100)-faceted, or *A*-type, step; and the (111)-faceted, or *B*-type, step [see Fig. 1(a)] [2]. These close-packed *A*- and *B*-type steps dominate the periphery of the islands on an fcc(111) surface. As shown previously in experimental studies of Pt/Pt(111) growth, hexagonal islands with a ratio of step lengths $L_A/L_B = 0.65$ are obtained at sufficiently high growth temperatures, irrespective of the kinetic

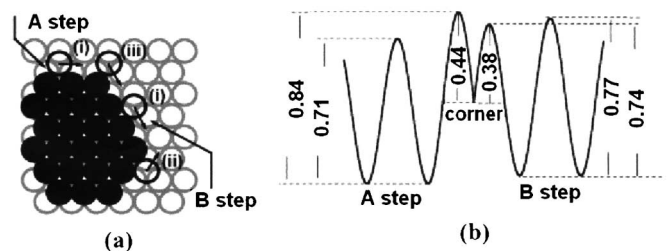


FIG. 1. (a) Illustration of the *A*- and *B*-type steps on Pt(111), and the three elemental rate processes controlling the redistribution of atoms around the periphery of an island: (i) edge-to-edge diffusion, (ii) edge-to-corner diffusion, and (iii) corner-to-edge diffusion. (b) The energy barriers used in the simulations of clean growth, as adopted from Ref. [10].

growth pathways [2]. This observation and subsequent theoretical studies [11] both indicate that a hexagon with alternating long and short edges is the equilibrium shape for the islands at sufficiently high temperatures. Therefore, the triangular islands of different orientations must be kinetically limited structures formed at the lower growth temperatures, and attempts to understand their formation mechanisms should accordingly be based on consideration of kinetic diffusion processes during growth.

In considering the redistribution of atoms along the periphery of an epitaxially growing island on fcc(111), three elemental atomic rate processes need to be emphasized: (i) edge-to-edge (or simply edge) diffusion, with an activation energy $E_{2\rightarrow 2}$; (ii) edge-to-corner diffusion, with $E_{2\rightarrow 1}$; and (iii) corner-to-edge diffusion, with $E_{1\rightarrow 2}$. For a given type of step, we generally expect $E_{1\rightarrow 2} < E_{2\rightarrow 2} < E_{2\rightarrow 1}$, because lowering coordinations normally would cost more energy [10]. We note that compact islands can be formed only when atoms can frequently travel from one edge to a neighboring edge by crossing the island corner [7]. We should also expect an intrinsic anisotropy in each of the three elemental rate processes, and rather than guessing at the sign of the anisotropy in a pair of rates, we adopt such activation energies strictly from first-principles calculations [9]. Those energy parameters are shown in Fig. 1(b), with (i) $E_{(2,A)\rightarrow(2,A)} < E_{(2,B)\rightarrow(2,B)}$; (ii) $E_{1\rightarrow(2,B)} < E_{1\rightarrow(2,A)}$; and (iii) $E_{(2,B)\rightarrow 1} < E_{(2,A)\rightarrow 1}$. Our explorations have shown that small variations in the values of these energy barriers will not change any of the major qualitative conclusions reached in the present study, as long as the variations do not alter the direction of any of the three rate anisotropies [12].

In our KMC simulations, we start with a seed of a minimal regular hexagon formed by seven atoms, placed at the center of a triangular 200×200 lattice; then we deposit every new atom randomly onto the lattice and allow it to make random walks. When an atom reaches the island it will continue to diffuse along the island periphery by the three elemental rate processes described above. We restrict ourselves to the temperature regime where no atom detachment from a straight segment of an island edge back to the terrace is allowed, because such processes correspond to higher activation barriers than the three elemental processes described above [13]. Atom detachment from a onefold coordinated corner site can easily take place within the growth temperature range of interest. Nevertheless, whereas such atom “leaking” events in principle signify the onset of island coarsening [7], they have little effect on the selection of the island shapes [12] and can therefore be suppressed. Furthermore, we apply the more stringent restriction that an adatom with three or more in-plane nearest neighbors become a static part of the island. This restriction not only enables one to better elucidate the delicate physics controlled by the three elemental atomic processes, but it is also physi-

cally accessible, because rate processes involving such initially more tightly bound atoms are still about (0.12–0.15) eV higher than those for the three elemental processes [8,12]. In all the simulations reported here, the deposition flux is fixed at 0.04 ML/s, which guarantees that no new island will be nucleated in the simulation cell. We have chosen the prefactors for all the hopping events to be uniquely $\nu = 4.2 \times 10^{10}T$, with T given in degrees K. Finally, our simulation terminates when the island size reaches 3000 atoms, which is large enough to show the overall island shape clearly.

The islands obtained in clean growth of Pt/Pt(111) at different temperatures are shown in Fig. 2. These islands are all nearly triangular, with no shape transition during the whole temperature range explored. Those results, in complete qualitative agreement with the recent experimental observations at clean growth conditions [3], are obtained for the first time from KMC simulations in which all the relevant energy barriers are from first-principles calculations for the same system of Pt/Pt(111) [9], without any tuning. We should also emphasize that, whereas reliable *ab initio* calculations are essential in providing the critical energy parameters, it is nontrivial, if not impossible, to conjecture on the island shape evolution during growth without carrying out such KMC simulations.

The above simulation results suggest that the energy barriers obtained by Feibelman are reliable enough in producing the qualitatively correct shape and orientation of the Pt islands on Pt(111). But precisely what is the crucial physical factor which selects the predominantly *B*-step bounded triangular islands out of all other possibilities? As shown previously, the triangular shape of the islands, in particular, their orientation, cannot be selected by the anisotropy in the edge diffusion barriers [6,8]. We have reconfirmed this point here by showing that, when the values of $E_{(2,A)\rightarrow(2,A)}$ and $E_{(2,B)\rightarrow(2,B)}$ are interchanged with all the other parameters fixed and a detailed balance among the various rates is maintained, we obtain triangular islands with the same orientation, as shown in Fig. 3(a) for the case of 455 K. Qualitatively, faster edge diffusion means that an adatom will visit the sites near the corners more frequently, but it will also reside for a shorter period of time during each visit, the balance of the two making the edge diffusion anisotropy

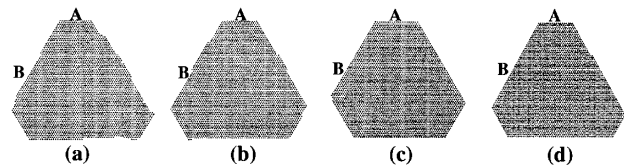


FIG. 2. Simulated island shapes obtained in “clean” growth at different growth temperatures: (a) 455 K, (b) 555 K, (c) 600 K, and (d) 650 K. The deposition fluxes in all the cases are fixed at 0.04 ML/s, and each island contains 3000 atoms.

unimportant. We next consider the possibility suggested by Ovesson *et al.* [8], namely, the inversion of the anisotropy in the corner-to-edge barriers could switch the orientation of the triangular islands. We have checked this suggestion by switching the values of $E_{1 \rightarrow (2,A)}$ and $E_{1 \rightarrow (2,B)}$ with all the other parameters kept fixed and found this suggestion invalid in the present case, as indicated by the simulation result shown in Fig. 3(b). Finally, we have inverted the anisotropy in the edge-to-corner barrier by switching the values of $E_{(2,A) \rightarrow 1}$ and $E_{(2,B) \rightarrow 1}$ and found that, with all other parameters kept fixed, an inverted triangular island bounded mainly by *A*-type steps is obtained [see Fig. 3(c)].

The above explorations lead to the following important generic conclusion. Unlike the fractal growth regime where many incoming adatoms would arrive at the island corner sites (or, equivalently, at the apexes of the growing fingers [14,15]) from the terrace, in the compact growth regime, only very few corner sites exist, and most adatoms arrive at the edges of the islands. Therefore, it is the delicate redistribution of the edge atoms that dictate the shape evolution as well as the overall orientation of the compact islands, rather than the redistribution of the relatively few corner atoms [8]. When this rationale is specified to the case of Pt(111), an atom reaching an *A* edge is less likely to escape from the edge through a corner site, but it is more likely to be joined by an atom reaching a neighboring *B* edge, thereby initiating the suicidal growth of the *A* edge. Here the corner-to-edge diffusion anisotropy is unimportant, also because at the temperatures where the rate-limiting edge-to-corner diffusion processes are active, even the slower one of the two corner-to-edge diffusion processes is already frequent.

Now we turn to the case of CO-induced growth. As reported recently, when the concentration of CO is increased, the *B*-step bounded triangular islands will change their shape first to irregular hexagonal islands, then to inverted triangular islands bounded by the *A*-type steps [3]. How does CO affect the surface processes

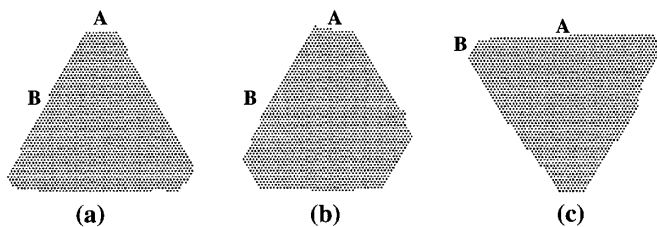


FIG. 3. Dependence of the triangular island orientation on the direction of the disparity in one of the three elemental rate processes introduced in Fig. 1(a). (a) and (b) show that reversing the disparity in either the edge-to-edge diffusion rates or the corner-to-edge diffusion rates has no effect on the island orientation. An inverted triangular island is obtained only by reversing the disparity in edge-to-corner diffusion rates, as shown in (c).

mentioned above, leading to the inversion of the triangular islands? Based on our understanding of the selection mechanism of the triangular islands in the clean case, we naturally expect that CO might reverse the anisotropy in the key edge-to-corner rate processes. This possibility becomes most feasible if we recall that CO preferentially adsorb at the upper edge of the *A*-type steps [16,17], tilting towards the lower-terrace side [see Fig. 4(a)]. Therefore, the decoration of CO at the *A*-type steps should weaken the binding strength of a Pt atom at the *A* step [3], in particular, at or near the lower edges of the step where the upper edges have been blocked by CO molecules. Quantitatively how much the binding energy is weakened can be obtained from first-principles calculations (see below). But before doing so, based on the very fact that the orientation of the triangular Pt islands is inverted in the presence of sufficient CO, we postulate that the preferential decoration of the *A* steps by CO will weaken the binding energy of Pt at the *A* steps to the degree that the edge-to-corner rate anisotropy is effectively reversed.

In simulating the effects of CO, we have explored two different schemes. First, we assume that the preference of the *A* steps by CO is so strong that only *A* steps are decorated. In this case, the binding energy lowering has a lower bound of $\Delta E_{A,CO} > 0.1$ eV in order to cause a reversal in the edge-to-corner rate anisotropy. We have taken a value of $\Delta E_{A,CO} = 0.14$ eV in our simulations, as shown in Fig. 4(b). We also assume that the CO molecules are randomly distributed along the *A* steps, corresponding to the known fact of fast CO diffusion along the steps (much faster than Pt adatom diffusion along the steps) [18]. We keep all the other energy barriers the same as obtained in Ref. [9]. The results are shown in Fig. 5. Figure 5(a) shows that the islands obtained at $\theta_{A,CO} = 0.02$ are still triangles bounded mainly by the *B* steps, as in the clean growth case. The transition from a triangular to a hexagonal shape takes place at $\theta_{A,CO} = 0.08$, as shown in Fig. 5(b). When the CO concentration is 0.3, the islands are still hexagonal, but with $L_A > L_B$, as shown in Fig. 5(c). Figure 5(d) shows the triangular island shape bounded predominantly by the *A* steps when the CO concentration is further increased to 0.8. Saturation of the CO effect is reached at the CO concentration of 0.8,

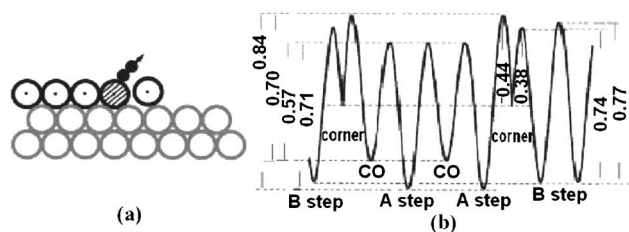


FIG. 4. (a) Schematic representation of the CO adsorption geometry at a step on Pt(111): The molecule is tilted towards the lower-terrace side, thereby weakening the binding strength of a Pt atom at the step, as shown in (b).

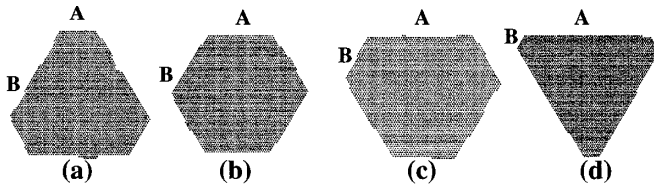


FIG. 5. Simulated island shapes at different concentrations of CO at the A steps: (a) 0.02, (b) 0.08, (c) 0.3, and (d) 0.8. The growth temperature is 455 K for all the coverages.

because there is no longer any shape change for $\theta_{A,CO} > 0.8$. These simulation results vividly demonstrate the beautiful transition in the Pt island shapes caused by an increasing concentration of the CO molecules decorated at the A steps, provided that the adsorption of CO reverses the intrinsic edge-to-corner rate anisotropy.

In the second scheme, occupations of both the A and B steps are considered, but with different populations given by $\theta_{A,CO}/\theta_{B,CO} = e^{\Delta E_{AB}/kT}$, where ΔE_{AB} is the binding energy difference of CO at the A and B steps, respectively, and k is the Boltzmann constant. We adopt the value of $\Delta E_{AB} = 0.1$ eV, obtained at a moderate coverage of CO at the steps [19]. Furthermore, we choose the same binding energy weakening of $\Delta E_{CO} = 0.14$ eV at both the A and B steps. Using these parameters, we have obtained essentially the same sequence of island shape evolution as shown in Fig. 5 as the coverage increases [12].

In order to verify the important postulate that the decoration of an A-type step by CO will weaken the binding energy of a Pt adatom at the step by at least 0.1 eV, we have carried out first-principles calculations using VASP [20] with its ultrasoft pseudopotential database and the generalized gradient approximation of the exchange-correlation potential. Here we must note that, even the state-of-the-art first-principles calculations were still unable to predict unambiguously whether the preferred binding site of a CO molecule is the bridge or the atop position along either step [19]. Fortunately, our goal is to determine the binding energy *change* of a Pt adatom at either site due to the presence of CO, rather than to provide a reliable answer for the preferred CO binding site. We find the binding energy weakens in all cases investigated, but by a different amount: Along step A, it weakens by 0.41 eV if the atop sites are occupied by CO, and by 0.59 eV if the bridge sites are occupied; along step B, it weakens by 0.32 and 0.66 eV if the atop and bridge sites are occupied, respectively. Most significantly, the weakening due to the preferential CO decoration of either site along the A step is clearly much larger than the minimum value of 0.1 eV required to reverse the edge-to-corner rate disparity. Such a reversal is more dramatic when the CO molecules mainly occupy the bridge sites, causing the island shape changes taking place at relatively lower CO coverages [12].

In summary, we have developed a unified picture for the selection of two-dimensional island shapes in Pt(111) homoepitaxy without or with the presence of minute amounts of CO adsorbates. For clean growth, we have shown for the first time that, when the energy barriers are rigorously adopted from first-principles calculations [9], only triangular islands of a fixed orientation are obtained within a wide range of growth temperatures. The orientation of the triangular islands is uniquely determined by the edge-to-corner rate anisotropy. The novel picture developed here for the case of clean growth is not only consistent with recent experiment, but it is also corroborated by the overall qualitatively correct predictions of the island shape evolution in the presence of CO.

We thank Thomas Michely, Peter Feibelman, and Shudun Liu for their careful readings of the manuscript and for helpful suggestions. This research was supported by the Natural Science Foundation of China, by Oak Ridge National Laboratory, managed by UT-Battelle, LLC, for the U.S. Department of Energy under Contract No. De-AC05-00OR22725, and by the U.S. National Science Foundation (Grant No. DMR-0071893).

- [1] R. Kunkel, B. Poelsema, L. K. Verheij, and G. Comsa, *Phys. Rev. Lett.* **65**, 733 (1990).
- [2] T. Michely, M. Hohage, M. Bott, and G. Comsa, *Phys. Rev. Lett.* **70**, 3943 (1993).
- [3] M. Kalf, G. Comsa, and T. Michely, *Phys. Rev. Lett.* **81**, 1255 (1998).
- [4] K. Kyuuo and G. Ehrlich, *Phys. Rev. Lett.* **81**, 5592 (1998); **84**, 2658 (2000).
- [5] S. D. Liu, Z. Y. Zhang, G. Comsa, and H. Metiu, *Phys. Rev. Lett.* **71**, 2967 (1993).
- [6] J. Jacobsen, K. W. Jacobsen, and J. K. Nørskov, *Surf. Sci.* **359**, 37 (1996).
- [7] Z. Y. Zhang and M. G. Lagally, *Science* **276**, 377 (1997).
- [8] S. Ovesson, A. Bogicevic, and B. I. Lundqvist, *Phys. Rev. Lett.* **83**, 2608 (1999).
- [9] P. J. Feibelman, *Phys. Rev. B* **60**, 4972 (1999).
- [10] We note an exception in Ref. [9], where $E_{(2,B) \rightarrow 1} < E_{(2,B) \rightarrow (2,B)}$.
- [11] G. Boisvert, L. J. Lewis, and M. Scheffler, *Phys. Rev. B* **57**, 1881 (1998).
- [12] J. Wu *et al.* (to be published).
- [13] G. Siswanto-Sun, Ph.D. thesis, University of Washington, 2000.
- [14] W. W. Mullins and R. F. Sekerka, *J. Appl. Phys.* **34**, 323 (1963).
- [15] Z. Y. Zhang, X. Chen, and M. G. Lagally, *Phys. Rev. Lett.* **73**, 1829 (1994).
- [16] D. M. Collins and W. E. Spicer, *Surf. Sci.* **69**, 85 (1977).
- [17] M. A. Henderson, A. Szabó, and J. T. Yates, Jr., *J. Chem. Phys.* **91**, 7245 (1989).
- [18] J. E. Reutt-Robey *et al.*, *Phys. Rev. Lett.* **61**, 2778 (1988).
- [19] P. J. Feibelman *et al.*, *J. Phys. Chem. B* **105**, 4018 (2001).
- [20] G. Kresse and J. Hafner, *Phys. Rev. B* **47**, 558 (1993); **49**, 14251 (1994).